Volume 2 | Number 31 | 21 August 2014 | Pages 12077–12602

# Journal of Materials Chemistry A

Materials for energy and sustainability

www.rsc.org/MaterialsA

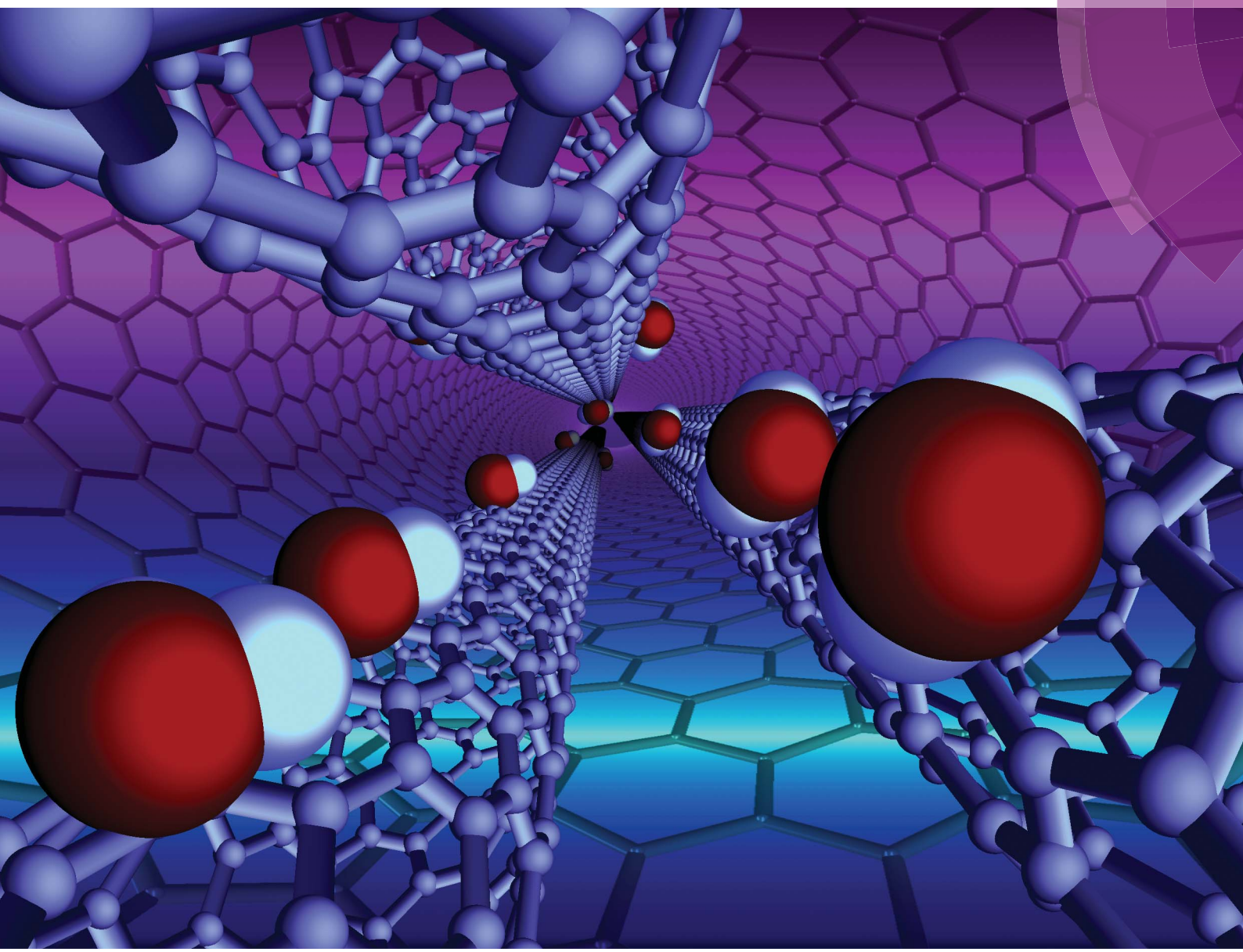

ISSN 2050-7488

ROYAL SOCIETY OF CHEMISTRY

PAPER

Xiaohua Zhang, Zhaohui Yang *et al.*

Enhanced water flux in vertically aligned carbon nanotube arrays and polyethersulfone composite membranes

Journal of Materials Chemistry A

PAPER

# Enhanced water flux in vertically aligned carbon nanotube arrays and polyethersulfone composite membranes†‡

Cite this: *J. Mater. Chem. A*, 2014, **2**, 12171

Shaoyun Li,[ac] Gaomin Liao,[ac] Zhipeng Liu,[ac] Yuanyuan Pan,[ac] Qiang Wu,[ab] Yuyan Weng,[c] Xiaohua Zhang,*[c] Zhaohui Yang*[c] and Ophelia K. C. Tsui[d]

Received 29th April 2014
Accepted 22nd May 2014

DOI: 10.1039/c4ta02119c

www.rsc.org/MaterialsA

We describe a novel preparation concept for a unique class of high-flux ultra-filtration membrane comprising a pre-aligned multi-walled carbon nanotube (MWCNT) array and polyethersulfone (PES). This membrane contains vertically aligned CNTs uniformly distributed inside a PES matrix. The vertically oriented water transportation pathway along the CNTs is verified to facilitate a dramatic enhancement in the water flux through the membrane. The water transportation speed increases about 3 times over the simply mixed CNT/PES membrane with random orientation and more than 10 times over the pure PES membrane under the same pressure load. Low working pressures as well as good retention properties enable this new composite membrane to be an ideal candidate for the future design of a highly efficient filtration membrane. This facile technique can potentially be applied to other filtration membrane systems to improve the separation efficiency.

## Introduction

With increasing concern about the growth in world population and limitation in water supply, there is an increasing drive in the water purification industry to find more efficient ways to increase the water supply for human use.[1,2] Filtration techniques by membranes have been deemed more cost and energy effective than other separation methods, such as distillation or absorption.[1,3] The ideal membrane system should possess an excellent stability under a wide range of processing conditions, high selectivity and produce a high mass flux with minimal driving force.[1,2,4] To achieve this goal, both the composition and structure of the membrane are key.

Carbon nanotubes (CNTs) with a one-dimensional tubular structure have been applied as direct filters[5–7] or effective additives[8,9] to improve membrane performances such as permeability, rejection, disinfection and antifouling behavior. A direct CNT filter is made up of vertically aligned CNTs with open ends extending out of the membrane plane, embedded in insulated inorganic or organic fillers.[5–7] Nanometer sized CNT hollow pores and smooth hydrophobic graphitic walls were hypothesized to serve as the frictionless path for the ultrafast mass transportation (shown as mechanism 3 in Scheme 1).[10,11]

[a]*Department of Polymer Science and Engineering, College of Chemistry, Chemical Engineering and Materials Science, Soochow University, Suzhou, 215006, P.R. China. E-mail: yangzhaohui@suda.edu.cn; zhangxiaohua@suda.edu.cn*

[b]*Physics Department, Soochow University, Center for Soft Condensed Matter Physics and Interdisciplinary Research, Suzhou, 215006, P.R. China*

[c]*Center for Soft Condensed Matter Physics and Interdisciplinary Research, Soochow University, Suzhou, 215006, P.R. China*

[d]*Physics Department, Boston University, Boston, MA, 02134, USA*

† This work is dedicated to Professor Weixiao Cao, Peking University, China, for his 80th birthday in November 2014.

‡ Electronic supplementary information (ESI) available: Evaluation of membrane performance, porosity measurement, schematic representation of the enhanced water transportation in different CNT blended membranes (Scheme S1), schematic diagram of the device for permeation tests (Scheme S2), TEM images of as-prepared CNTs (Fig. S1), SEM images of the surface morphology of three types of CNT/PES membranes (Fig. S2), TGA and SDT analysis of the R-CNT/PES film and the VA-CNT/PES film (Fig. S3), Raman (Fig. S4) and FTIR (Fig. S5) spectra of the blend membrane and standard curves of PEG 20 000 with iodine staining (Fig. S6). See DOI: 10.1039/c4ta02119c

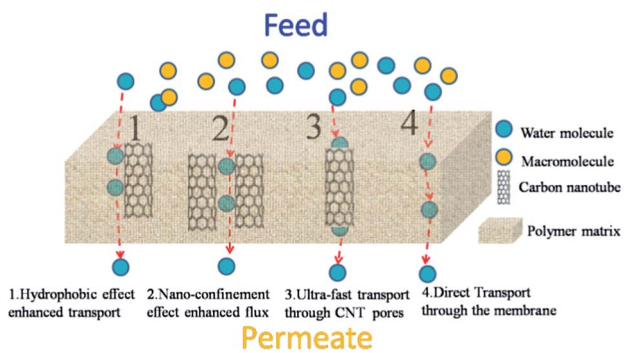


Scheme 1 Illustration of possible pathways for water transportation in a CNT/polymer blend membrane due to (1) hydrophobic effect enhanced transport, (2) nano-confinement enhanced flux, (3) ultrafast transport through the CNT pores, and (4) direct transport through the membrane matrix.[15]

The water flux rate has been experimentally measured to be 3–4 orders of magnitude faster than the conventional flow estimated from the Hagen–Poiseuille equation.[6,7] The enhancement was attributed to the ballistic motion of water chains (1D wire) inside the CNTs due to the strong hydrogen bonding between the water molecules and minimal interaction with the CNT inner wall.[12,13] However, such vertically aligned CNT filters (referred to as VA-CNT filters) require very high quality CNTs (without any impurity blockage inside the tubes) and complicated end-opening techniques (*e.g.* plasma etching or argon milling). It is hence not economical for scalable synthesis compared with the conventional mixed matrix membranes.[14]

Meanwhile diffusion along the external surface of the CNTs can also speed up water transportation *via* a hydrophobic effect (shown as mechanism 1 in Scheme 1) or a nano-confinement effect (mechanism 2).[15] Given the possible mechanisms for water transportation shown in Scheme 1, both the miscibility between CNTs and the polymer fillers and the interaction between the water molecules and the CNT external walls should affect the membrane permeability.

It has been predicted that the permeation coefficient is correlated with the aspect ratio of the CNTs and CNT fraction.[16] In principle, one may attain high permeability by using CNTs with high aspect ratio in large volume fraction. Unfortunately, CNT aggregation always presents a serious problem whether in the mixing of CNTs in a solution or a melt mixture due to the strong van der Waals interaction between the CNTs. Pre-surface modifications of the CNT are thus necessary to improve the compatibility. The relevant effects on the performance of the pre-modified-CNT based composite membrane have been well studied in the literature.[17–20] However, the conventional pretreatment techniques (*e.g.* acid oxidation treatment) often shorten the length of the CNTs and destroy the external graphitic walls. The rough and hydrophilic CNT surface may thus trap the water molecules and slow down their motion. The reduced aspect ratio of the shortened CNTs is also unfavorable to the membrane performance.[16]

Relatively few efforts have been made to prove the performance of CNT/polymer blend membranes by taking advantage of the well-known orientation effects of CNTs towards permeability. The most efficient pathway of the CNT blended membrane is predicted when all the CNTs are perpendicular to the membrane plane.[4,14] By using the finite element method, Gusev *et al.* concluded that the aligned CNTs could accelerate the mass transportation along the CNT direction.[16] In our previous study, the aligned CNT array/hydro-gel system showed an ultra-fast wetting/dewetting behavior,[21] which implies enhanced water transportation and lends support to the concept. Unfortunately, it is a challenge to control the orientation of CNTs in a polymer matrix.[2,14] Dielectrophoresis[22] and special filtration techniques[23] can help align the CNTs. However the complicated pre-chemical modification process and relatively low CNT loading impede their developments.

Here we introduce a new strategy to synthesize a high-flux ultra-filtration membrane based on vertically aligned CNT arrays and polyethersulfone (PES) (referred to as VA-CNT/PES films) through a simple drop-casting and phase inversion process. The well-aligned arrays of CNTs in the PES matrix are uniformly distributed in the membrane. The PES components exhibit excellent macromolecule (PEG-20 000) rejection properties. The water flux in such a VA-CNT/PES composite film is measured to be 3 times faster than the CNT/PES membrane in which the CNTs are randomly distributed (referred to as R-CNT/PES films) and 10 times faster than the pure PES membrane under the conditions. Such enhancement in flux is also obtained when the feeding is a PEG-20 000 solution during the retention property test. Excellent retention properties and stable separation behavior are also found in the VA-CNT/PES membranes. In the following, we shall present data demonstrating these attributes and detail the structure and surface properties of these membranes by SEM, TGA, FTIR and contact angle measurements.

Compared to the direct VA-CNT filters, our system does not require a complicated CNT end-opening procedure. The retention properties rely on the polymer matrix which is convenient to connect with the technologies currently used in the membrane industry. More importantly we can obtain well distributed and aligned CNTs without any pre-modification or post-treatment. Also this technique does not damage the CNT external walls or cause a decrease in the aspect ratio of the CNTs. The well aligned CNTs form a highly efficient water pathway which facilitates an enhanced water flux and lower pressure consumption. The density and length of the CNTs can be controlled by the CNT growth parameters which may further improve the membrane performance. The new method presented here may shed light on the design of future CNT blend membrane systems.

## Results and discussion

The vertically aligned CNTs obtained here through the CVD method are 130 ± 30 μm in height with an outer diameter of around 15 nm. (Corresponding TEM images are shown in ESI Fig. S1.†) Fig. 1 presents the SEM cross-section images of the VA-CNT/PES film (Fig. 1a and d), R-CNT/PES film (Fig. 1b and e) and pure PES film (Fig. 1c and f). For ease of comparison, we

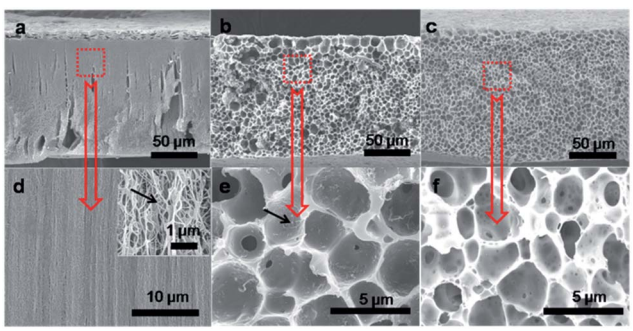


Fig. 1 The SEM cross-section images of the CNT/PES composite membranes under different magnifications, (a and d) VA-CNT/PES film; (b and e) R-CNT/PES film; (c and f) pure PES film; the black arrow in the inset of (d) shows the magnified free space between the CNTs; another black arrow in (e) indicates the isolated carbon nanotubes in the PES matrix.

chose three kinds of films with a similar thickness of around 150 μm. As Fig. 1b shows, the R-CNT/PES film has many macro-void holes with diameters of 5–10 μm due to the phase-inversion process, commonly found in the literature.[27] In the magnified image (Fig. 1e), one can see that the CNTs are randomly dispersed inside the PES matrix (as indicated by the black arrow). In the case of the pure PES film (Fig. 1c and f), similar macro-void structures form across the whole film. This suggests that addition of the hydrophobic CNTs does not significantly influence the phase inversion behavior of PES. However, a quite different structure is found in the case of the VA-CNT/PES film. As Fig. 1a shows, two distinctive layers are discernible, indicative of a thin-film composite (TFC) system. We find that the top surface layer with a thickness of 10 ± 5 μm is composed of PES having the same macro-void structure as the pure PES membrane. The bottom thick layer with a thickness of about 130 μm is a mixture of PES and an aligned CNT array. The absence of macro-void structures indicates that the phase inversion process does not occur in the bottom layer. One possible explanation is that the superhydrophobic VA-CNT array suppresses the phase inversion which causes the formation of macro-voids. From the magnified image shown in Fig. 1d, the vertically aligned CNTs penetrate the whole membrane, forming a nearly ideal filtration membrane structure as discussed above. As seen in the inset of Fig. 1d, an interconnected network of CNTs exists inside the PES matrix. There are still spaces between the CNTs and polymers with a distance of sub-hundred of nanometers (as indicated by the black arrow). We speculate that both the vertically aligned CNT structure and spaces between the CNTs and polymers contribute to the enhancement in flux that will be discussed below.

### Thermal and spectra analysis

The thermal decomposition analyses of VA-CNT/PES (dashed line) and R-CNT/PES (solid line) blend films are shown in ESI Fig. S3.† Similar weight-loss curves in TG graphs and the same peak position in the DTG (derivative thermogravimetry) curves demonstrate a similar thermal stability and CNT loading of two films. This verifies a similar chemical nature of the CNTs and the PES fillers in the two membrane systems. From the Raman spectra shown in ESI Fig. S4,† a higher $G/D$ ratio is found in the R-CNT/PES film compared with the VA-CNT/PES film, which indicates a better crystallized graphitic wall in the unmodified commercial CNTs. Fig. S5† shows the FT-IR spectra of three types of films. The characteristic vibration peaks at 1587 $cm^{-1}$ and 1657 $cm^{-1}$ correspond to the graphitic band of CNT and PES, respectively. No characteristic peaks related to the carboxylic or ester groups are shown in these films. It indicates that there is no chemical bonding between the CNTs and the PES fillers.

### Contact angle measurements

Fig. 2 shows the contact angle measurement for three types of CNT/PES membranes. Due to the existence of hydrophobic unmodified CNTs in the R-CNT/PES film, the contact angle of the R-CNT/PES film is 85 ± 5°. The value for the pure PES film is 74°, which is consistent with reported values.[19] The contact angle of the VA-CNT/PES film is 65 ± 3°, indicating the most hydrophilic surface. It is quite abnormal because the as-prepared CNT array is super-hydrophobic, which cannot increase the hydrophilicity of the membrane. It is well known that the surface roughness will affect the wettability of the film.[28] However the surface morphology of the three types of membranes is quite similar from the SEM observations (see ESI Fig. S2†), which should not significantly influence the surface properties. Such a decrease in the contact angle, which can benefit fast water transportation, might be caused by the formation of a well aligned CNT structure in the membrane matrix. In our previous work, composite films consisting of a

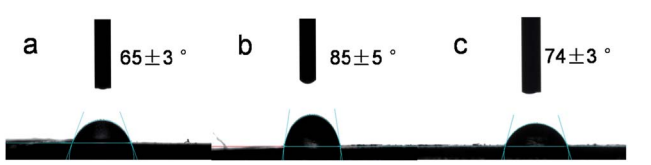


Fig. 2 Contact angle measurements of three kinds of membranes: (a) VA-CNT/PES membrane with 65 ± 3°; (b) R-CNT/PES membrane with 85 ± 5°; (c) pure PES membrane with 74 ± 3°.

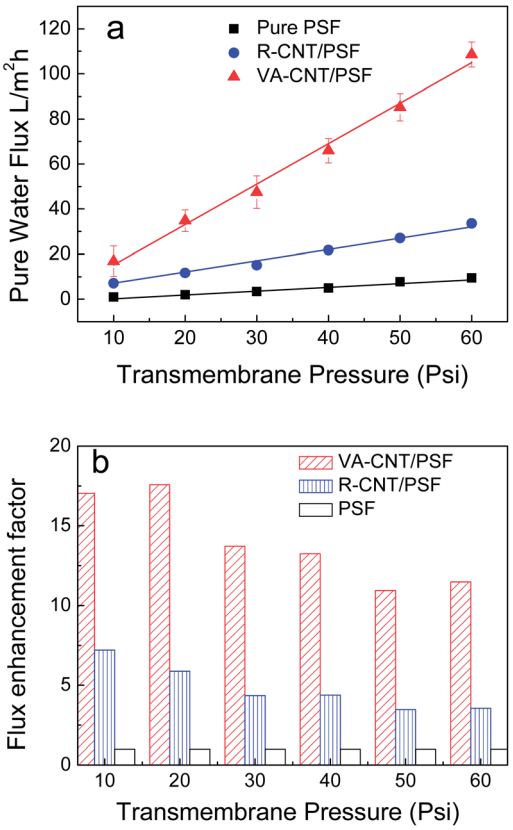


Fig. 3 (a) Pure water flux of the VA-CNT/PES (triangles), R-CNT/PES (circles) blend membrane and pure PES membrane (squares) as a function of working pressure. (b) The flux enhancement factor in the different types of CNT/PES membranes at different working pressures (the flux in the pure PES membrane is set as the standard).

vertically aligned CNT array in a hydro-gel matrix also exhibited a small contact angle with fast wetting and dewetting ability.[21]

### Membrane filtration performance

Fig. 3 shows the pure water flux as a function of the trans-membrane pressure in the three types of films under the same test conditions. All these samples, the VA-CNT/PES (triangles), R-CNT/PES (circles) and pure PES membranes (squares) show a good linear relationship between flux and pressure. Compared with the pure PES film, the R-CNT/PES film shows a water flux enhancement factor of 3–7 which is close to a previous report.[20] It should be emphasized that the CNTs used in the literature have a pre-oxidation treatment that improves the hydrophilicity of the CNTs. Our CNTs are not pre-treated, so the flux increase should be caused by the hydrophobic effect and increase in porosity.[15,19] The extreme hydrophobic surface of the CNTs prevents the water molecule from wetting the polymer pores thus leads to a faster transport of water. Also the water molecules may hop from one site to another by interacting with the CNT surfaces due to the rapid sorption and desorption capacity of CNTs,[15] which leads to a fast transport of water molecules along the CNT surface. More importantly, the VA-CNT/PES film exhibits an even better water transportation ability as compared with the R-CNT/PES film. The flux enhancement factor of VA-CNT/PES membranes is calculated to be 2.4 to 3.3 (depending on the working pressure, see Fig. 3b) over the R-CNT/PES film and 10 to 17 (depending on the working pressure, see Fig. 3b) over the pure PES film under the same conditions. Theoretical simulations have predicted a flux enhancement factor of 3 for gas transportation caused by the alignment of CNTs.[16] In our case, the enhancement factor of the VA-CNT/PES film *versus* R-CNT/PES film is close to the simulation result.

Generally the water flux has a direct relationship with the membrane porosity.[29] The porosity of the R-CNT/PES film is (59 ± 5%), while the value for the pure PES is (40 ± 3%). Interestingly, the porosity of the VA-CNT/PES film is (52 ± 5%) although it does not show an obvious macro-void structure. This observation can be explained as the numerous nano-meter sized free spaces between the CNT array and the PES matrix (as shown in Fig. 1d).[21] Although the porosity of the VA-CNT/PES film is smaller as compared to the R-CNT/PES film, a flux enhancement (the flux enhancement factor is around 3) is observed in the VA-CNT/PES system. The acceleration mechanism is thus ascribed to the vertically aligned CNT structure as well as interconnected hydrophobic free spaces between the CNTs and polymer fillers rather than the porosity increase. It indicates water molecule transfer along these efficient pathways through the membrane with a relatively high speed as shown in Scheme 1.

The retention test is carried out on the same ultra-filtration cell with PEG-20 000 as the feeding solution. As Fig. 4a shows, the three kinds of films show a rejection property of 75–95% at different applied pressures. An optimized working pressure in the VA-CNT/PES film is 40 psi with a rejection rate of 95%. Under these conditions, the permeate flux in the VA-CNT/PES film is measured to be 3.7 times higher than the R-CNT/PES film

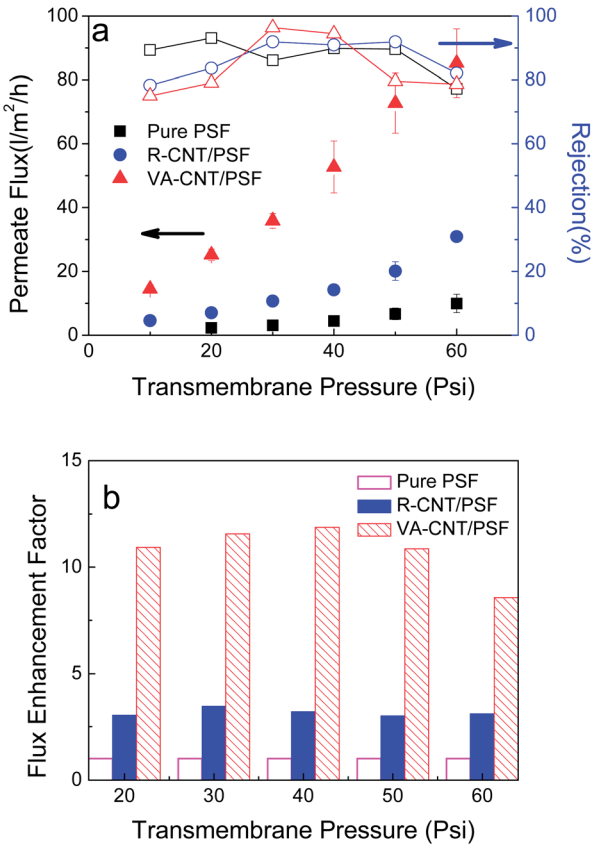


Fig. 4 (a) Water flux (left) and retention (right) behavior of the three kinds of membranes discussed in the text towards a 50 mg $l^{-1}$ PEG-20 000 solution, triangles: VA-CNT/PES, circles: R-CNT/PES, and squares: pure PES membrane. (b) Flux enhanced factor for the three kinds of membranes at different pressures. Sparse: VA-CNT/PES, solid: R-CNT/PES, hollow: pure PES membrane. The flux in the pure PES membrane is set as the standard.

and 12 times higher than the pure PES film. The mechanism of the enhancement is similar to that discussed above. Based on Fig. 4a, the rejection rate of the two CNT-containing films increases with increasing pressure and reaches a maximum at 30 psi whereas the pure PSF film shows the best retention performance at 20 psi. This phenomenon is similar to the observation by Choi *et al.* and probably caused by the PSF surface fouling of the PEG molecules.[18] It indicates the formation of a relatively compact PEG layer at higher operating pressure which probably suppresses the transport of the solute. The rejection rate then decreases with further increase in the applied pressure due to the increasing concentration polarization effect.[18] Meanwhile the permeate flux increases with the pressure monotonically but does not follow a linear relationship. This may be caused by the alternation of the pore structure under high pressure and change in the surface properties of the CNTs (*e.g.* the PEG molecules adsorbing onto the CNTs).

To test the durability of the composite membrane, we record the time sequenced permeate flux at a constant pressure of 40 psi. As Fig. 5 shows, the flux (solid labels) in the three types of the membranes decreases with time and eventually reaches an equilibrium value. The decrease in the flux after a 5 hour

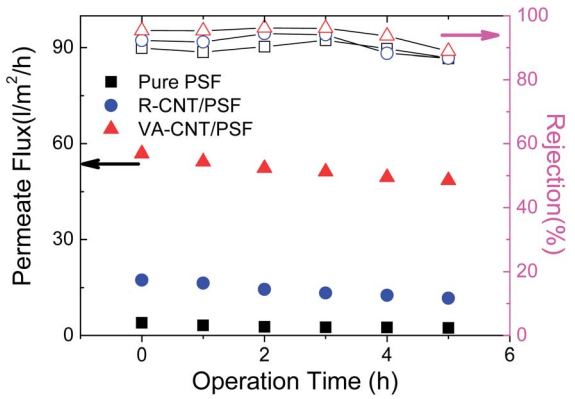


Fig. 5 Time sequenced permeate flux (solid symbols) and rejection (hollow symbols) of three types of PES membranes at the working pressure of 40 psi, VA-CNT/PES (triangles), R-CNT/PES (circles) and pure PES membrane (squares).

running is calculated to be 27% for the VA-CNT/PES film, 58% for the R-CNT/PES film and 81% for the pure PES film. As a smaller decrease of flux usually indicates a better anti-fouling ability,[30] the VA-CNT/PES film shows improved anti-fouling properties compared with the other two membranes. Meanwhile the rejection rate (hollow labels) maintains at a high constant level (around 90% for the R-CNT/PES film, 89% for the pure PES film and 95% for the VA-CNT/PES film) and only starts to decrease after 4 hours operation. The decrease of the flux can be ascribed to the adsorption of PEG molecules on the membrane surface which forms a cake-like layer during the permeation process.[30]

## Experimental section

### Materials

Polyethersulfone resin (PES, $M_w = 75\,000$ g mol$^{-1}$) was supplied by Acros Organics. Polyethylene glycol (PEG, $M_w = 20\,000$ g mol$^{-1}$) and polyvinylpyrrolidone (PVP, $M_w = 58\,000$ g mol$^{-1}$) were purchased from Aladdin Chemistry (Shanghai, China). MWNT powders were obtained from Shenzhen Nanotech Port, Shenzhen China (15 nm O.D., 5–10 μm in length). Other chemicals were obtained from Sinopharm Chemical Reagent (Shanghai, China) without further purification.

### Characterization

The morphology of the CNT/PES composite membranes was examined by scanning electron microscopy (Hitachi S-4700, Japan). Cross-sectional images were obtained after fracturing the membranes in liquid nitrogen. A Tecnai G220 (FEI) transmission electron microscope (TEM) operated at a 180 kV accelerating voltage was used.

A thermogravimetric analyzer (TGA) (SII EXSTAR TG/DTA 6300) was utilized to investigate the thermal weight loss of samples in a nitrogen environment by heating up to 800 °C with a heating rate of 20 °C min$^{-1}$.

The contact angle measurement was carried out on a contact angle goniometer (OCA20, Dataphysics, Germany) equipped with a video camera at room temperature to check the hydrophilicity of the membrane surface. Three samples were measured to obtain an average result.

The FTIR spectra were obtained using a Nicolet 6700 FT-IR spectrophotometer. The Raman spectra were measured on a Raman Spectrophotometer (HR800, HORIBA Jobin Yvon Company) excited by a laser with a wavelength of 632.8 nm.

### Preparation of the vertically aligned CNT array

The vertically aligned CNT array was grown through a conventional chemical vapor deposition (CVD) method with a Fe/Al thin film pre-deposited as the catalyst *via* E-beam evaporation.[24] The height and density of the array can be controlled by the growth parameters.

### Preparation of the R-CNT/PES, pure PES and VA-CNT/PES membranes

Preparation of the R-CNT/PES membrane is based on what is reported in the literature with some modification.[18,25] The precursor solution containing 14 wt% PES and 2 wt% PVP (used as the porogen) in *N*-methyl pyrrolidone (NMP) is continuously stirred for 2 hours to form a homogeneous solution. Then it is mixed with 1 wt% MWCNT powder followed by strong ultrasonication over 3 hours. After storing for 24 hours to remove air bubbles, 0.5 ml solution is drop-coated onto the surface of a 2 cm × 5 cm clean glass slide and then transferred to a coagulating water bath to obtain a free standing film. After thoroughly rinsing with DI water, the membrane is dried for 12 hours at room temperature and stored in DI-water for further test.

To prepare the pure PES membrane, the same amount of precursor solution (without CNTs) is drop-coated and treated with the same procedure.

To prepare the VA-CNT/PES membrane, 0.05 ml precursor solution (without CNTs) is drop-coated onto the surface of a CNT array film (about 1 cm × 1 cm in area) and treated with the same procedure as mentioned above. The VA-CNT/PES membrane is very easily peeled off from the silicon substrate after immersion in a coagulation bath.

### Porosity measurement

The membrane porosity is measured through the "dry-wet weight loss" method.[26] Details can be found in the ESI.†

### Membrane performance test

An ultra-filtration test system is designed as shown in ESI Scheme S2† to evaluate the filtration performance of the CNT composite membranes. All filtration experiments are conducted at a constant trans-membrane pressure between 10 and 60 psi with a system temperature of 20 °C. Each membrane is placed on a porous stainless steel disk with an active membrane area of 1.54 cm$^2$ for the pure PES membrane and the R-CNT/PES membrane and 0.38 cm$^2$ for the VA-CNT/PES membrane. Pure DI water and an aqueous solution of PEG-20 000 (50 mg L$^{-1}$) are used as the feedings. The data are recorded after 30 min

pre-treatment at the working pressure. Each film is tested at least for 5 samples to get an average result. Details of this experiment can be found in the ESI.†

## Conclusions

In conclusion, we have designed and fabricated a new type of ultra-filtration membrane based on the vertically aligned MWCNT array/PES composites. The uniqueness of this membrane is the orderly alignment of CNTs inside the polymer matrix which provides the ultra-efficient pathway for water transportation. The promising enhancement in the water flux verifies the theoretical prediction of the acceleration effect caused by the aligned CNTs. The good retention behavior and stable separation properties benefit the separation efficiency of this aligned CNT array/PES blend membrane. In future work, the array height and density, the CNT diameter as well as the surface properties will be precisely controlled to further improve the membrane performance. This technique might show potential for use in other ultra-filtration, nano-filtration and reverse osmosis systems.

## Acknowledgements

This work was financially supported by the National Basic Research Program of China (973Program) (no. 2012CB821505), National Natural Science Foundation of China (no. 91027040, 21204059, 21204058, 21274103, and 21104054), Natural Science Foundation of Jiangsu Province (no. BK2011300). The authors also thank for the Specially-Appointed Professor Plan in Jiangsu Province (no. SR10800312) and Project for Jiangsu Scientific and Technological Innovation team (2013). Prof. F. Zhu-ge, Mr B. Fu from Ningbo Institute of Materials Technology & Engineering (Chinese Academy of Sciences) and Mr L. Li from ULVAC (Suzhou) Co. LTD for the help with the E-beam evaporation experiment were also greatly acknowledged. We also thank Prof. J. Meng from Tianjin Polytechnic University for the helpful discussion.

## Notes and references

1 M. Elimelech and W. A. Phillip, *Science*, 2011, **333**, 712.
2 M. A. Shannon, P. W. Bohn, M. Elimelech, J. G. Georgiadis, B. J. Mariñas and A. M. Mayes, *Nature*, 2008, **452**, 301.
3 D. Li and H. Wang, *J. Mater. Chem.*, 2010, **20**, 4551.
4 M. T. M. Pendergast and E. M. V. Hoek, *Energy Environ. Sci.*, 2011, **4**, 1946.
5 B. J. Hinds, N. Chopra, T. Rantell, R. Andrews, V. Gavalas and L. G. Bachas, *Science*, 2004, **303**, 62.
6 M. Majumder, N. Chopra, R. Andrews and B. J. Hinds, *Nature*, 2005, **438**, 44.
7 J. K. Holt, H. G. Park, Y. Wang, M. Stadermann, A. B. Artyukhin, C. P. Grigoropoulos, A. Noy and O. Bakajin, *Science*, 2006, **312**, 1034.
8 C. H. Ahn, Y. Baek, C. Lee, S. O. Kim, S. Kim, S. Lee, S. H. Kim, S. S. Bae, J. Park and J. Yoon, *J. Ind. Eng. Chem.*, 2012, **18**, 1551.
9 S. Kar, R. C. Bindal and P. K. Tewari, *Nano Today*, 2012, **7**, 385.
10 G. Hummer, J. C. Rasaiah and J. P. Noworyta, *Nature*, 2001, **414**, 188.
11 A. Kalra, S. Garde and G. Hummer, *Proc. Natl. Acad. Sci. U. S. A.*, 2003, **100**, 10175.
12 A. Noy, H. G. Park, F. Fornasiero, J. K. Holt, C. P. Grigoropoulos and O. Bakajin, *Nano Today*, 2007, **2**, 22.
13 S. Joseph and N. R. Aluru, *Nano Lett.*, 2008, **8**, 452.
14 D. S. Sholl and J. K. Johnson, *Science*, 2006, **312**, 1003.
15 K. Gethard, O. Sae-Khow and S. Mitra, *ACS Appl. Mater. Interfaces*, 2010, **3**, 110.
16 A. A. Gusev and O. Guseva, *Adv. Mater*, 2007, **19**, 2672.
17 C. F. De Lannoy, E. Soyer and M. R. Wiesner, *J. Membr. Sci.*, 2013, **447**, 395.
18 J. H. Choi, J. Jegal and W. N. Kim, *J. Membr. Sci.*, 2006, **284**, 406.
19 S. Qiu, L. Wu, X. Pan, L. Zhang, H. Chen and C. Gao, *J. Membr. Sci.*, 2009, **342**, 165.
20 E. Celik, H. Park, H. Choi and H. Choi, *Water Res.*, 2011, **45**, 274.
21 Z. Yang, Z. Cao, H. Sun and Y. Li, *Adv. Mater.*, 2008, **20**, 2201.
22 S. Shekhar, P. Stokes and S. I. Khondaker, *ACS Nano*, 2011, **5**, 1739.
23 S. Kim, J. R. Jinschek, H. Chen, D. S. Sholl and E. Marand, *Nano Lett.*, 2007, **7**, 2806.
24 Z. Liu, G. Liao, S. Li, Y. Pan, X. Wang, Y. Weng, X. Zhang and Z. Yang, *J. Mater. Chem. A*, 2013, **1**, 13321.
25 S. Maphutha, K. Moothi, M. Meyyappan and S. E. Iyuke, *Sci. Rep.*, 2013, **3**, 1509.
26 Y. Ma, F. Shi, Z. Wang, M. Wu, J. Ma and C. Gao, *Desalination*, 2012, **286**, 131.
27 Y. Medina-Gonzalez and J. C. Remigy, *Mater. Lett.*, 2011, **65**, 229.
28 D. Quere, *Annu. Rev. Mater. Res.*, 2008, **38**, 71.
29 M. J. Han and S. T. Nam, *J. Membr. Sci.*, 2002, **202**, 55.
30 J. Yin, G. Zhu and B. Deng, *J. Membr. Sci.*, 2013, **437**, 237.

 